Vulnerability in a One-Dimensional Transmural Model of Human Ventricular Tissue in Heart Failure

S Kharche[1], AV Holden[2], H Zhang[1]

[1]Biological Physics Group, School of Physics and Astronomy, University of Manchester, Manchester, UK
[2]School of Biomedical Sciences, University of Leeds, Leeds, UK

Abstract

Heart failure (HF) induces remodeling in cellular ionic channel kinetics and calcium handling in the ventricle. In the present study, we investigated the effects of HF on rate dependent electrical activity of human ventricular myocytes by characterizing the dynamic action potential duration restitution (APDr), action potential (AP) alternans, intracellular calcium transient ($[Ca^{2+}]_i$) alternans, and delayed after depolarizations (DADs) AP. Conduction velocity restitution (CVr) and vulnerability window (VW) of homogeneous tissue to re-entry subject to DAD was investigated. Vulnerability of transmural ventricular strand was also quantified under normal (NF) and HF conditions.

1. Introduction

HF occurs with advancement of age, untreated hypertension, and coronary artery disease among other conditions. HF is associated with fatal cardiac arrhythmias [1]. Experimental studies have characterized HF-induced remodelling in cellular electrophysiology and intracellular Ca^{2+} handling of human ventricular myocytes, all of which have been incorporated into a mathematical model of electrical AP [2].

However, it is still unclear how HF affects the rate dependent electrical activity and thus ventricular excitation conduction in humans. Slope of APDr in cells has been related to conduction block and spiral instability in tissue [3 - 5]. The occurrence of AP alternans in cells has been related to heterogeneous conduction in human atrial tissue [6]. In conjunction with AP alternans, $[Ca^{2+}]_i$ alternans contribute to concordant and discordant conduction patterns in cardiac tissue [7]. Therefore in the present study we investigated the rate dependent properties of single cell models in the three cells types, *i.e.* endocardial (endo-), midcardial (mid-), and epicardial (epi-) [8]. We further quantified the vulnerability of homogenous tissue to re-entry subjected to DAD induced-APs. Effects of HF on APD heterogeneity and tissue's

vulnerability to the genesis of unidirectional conduction block on a transmural ventricular strand were also investigated.
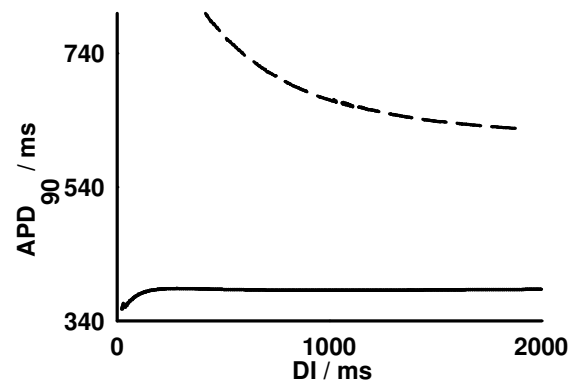
Fig 1. APDr for mid- cell in NF (solid line) and in HF (dashed line). In HF, the APDr has a negative slope.

2. Methods

Cell models for endo-, mid-, epi- were constructed by incorporating transmural differences as described in [8]. We simulated HF in cell and tissue models using an existing model for ventricular cells [1]. HF was simulated by reducing current density of transient outward current (I_{to}) by 64 %, of inward rectifier potassium current (I_{K1}) by 25 %, increasing sodium-calcium exchanger activity (I_{NaCa}) by 65 %, reducing activity of sodium potassium pump (I_{NaK}) by 42 %, increasing current density of background calcium current (I_{bCa}) by 34 %, and reducing current density of background sodium (I_{bNa}) current by 100 %. In addition, the Ca^{2+} uptake by the network sarcoplasmic reticulum (SR) was reduced by 33 %.

Cell models were paced at a constant basic cycle length (BCL) of 100 times. The ultimate APD (at 90 % repolarization, APD_{90}) and diastolic interval (DI) were noted to construct APDr curves. At low BCL, several of the final APs, defined as $V_m > -35$ mV, were noted as a

function of BCL to elicit AP alternans behaviour. Amplitude of $[Ca^{2+}]_i$ transients was noted simultaneously to elicit $[Ca^{2+}]_i$ alternans behaviour. DAD in cell models were elicited by simulating premature release of $[Ca^{2+}]_i$ in the SR after pacing 5 times at an interval of 1 s. Resulting membrane potentials were noted to investigate DAD induced AP.

The cell models were incorporated into a reaction diffusion partial differential equation (PDE) of 1-D virtual tissue, which takes the form

$$C_m \frac{\partial V}{\partial t} = -I_{ion} + D \frac{\partial^2 V}{\partial x^2}$$

where D is the diffusion constant with value 0.154 mm^2/ms to give a conduction velocity of 70.1 cm/s for a solitary wave in a 1-D epi- tissue. A time step of 0.02 ms and a space step of 0.2 mm were taken to obtain stable numerical solutions. The virtual ventricular strands were taken to be 15 mm long in accordance with the physiological thickness of the ventricular wall [8], unless otherwise stated.

CVr in 1-D homogenous tissues was investigated by applying 2 conditioning pulses at an interval of 1s, after which a premature stimulus was applied. Conduction velocity (CV) of the resulting propagation was measured as a function of the DI to construct CVr curves in homogenous strands of NF and HF tissues. Vulnerability to premature stimulus was quantified by applying 2 conditioning pulses after which a premature stimulus in the centre of the strand for a length of 0.8 mm was applied. The resulting propagation behaviour was noted to measure vulnerability window (VW) as described by [9]. Vulnerability in 1-D tissues of length 100 mm due to DAD was investigated by applying 5 conditioning pulses at 1 s intervals, and then simulating premature release of
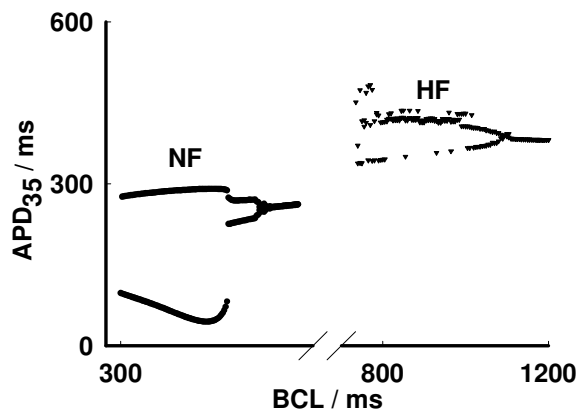
Fig 2. APD alternans bifurcation diagram in mid- NF and HF cell models. A break in the BCL axis was introduced to improve clarity.

SR $[Ca^{2+}]_i$ along a length of 10 mm (50 cells) in the centre of the tissues.

APD distribution in transmural tissues were computed as function of space. Spatial distribution of VW in transmural tissue was quantified using a similar stimulation protocol to the homogenous case.
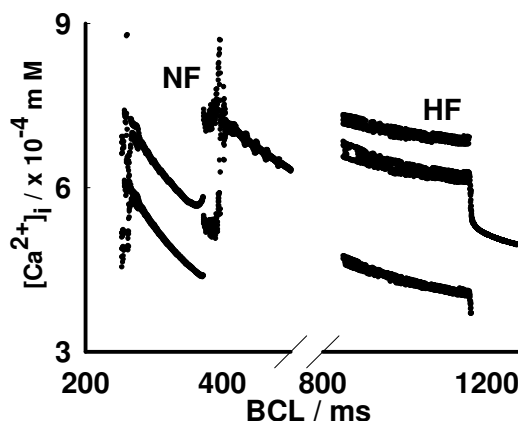
Fig 3. $[Ca^{2+}]_i$ alternans in mid- NF and HF cell models. The 2:2 response in the HF case is small as compared to NF. . A break in the BCL axis was introduced to improve clarity.

3. Results

After incorporating ionic remodelling changes due to HF we investigated each of the cell models for rate dependent behaviour. We illustrate all results with mid-cell and 1-D models.

In NF, we saw that for small DI, APDr was steep with a positive slope. Region of negative slope were seen in HF. This is illustrated in Fig 1 using the mid- case for NF and HF. For the three different cell types, the maximal slope was seen in the mid- model for both NF (0.94) and HF (-1.07).

Upon dynamically pacing the cell models at a fixed BCL, AP alternans occurred when BCL became sufficiently small and 1:1 response was abolished and a 2:2 response was observed (see for *e.g.* [10]). By plotting the small and large APD against BCL, a bifurcation diagram was constructed to show the existence of 2 or more distinct APD for the same BCL (or equivalently, pacing frequency). This is shown in Fig 2 for the mid-cases where AP alternans occur at much lower BCL in NF than in HF. The results for the other types of cell models show a similar pattern. In NF, AP alternans occur at or below a BCL of 405 ms for endo-, 394 ms for mid-, and 390 for epi-. For HF, AP alternans occur at or below a BCL of 765 ms for endo-, 1110 ms for mid-, and 675 ms for epi-.

At low BCL, $[Ca^{2+}]_i$ alternans *i.e.* for a given BCL, the
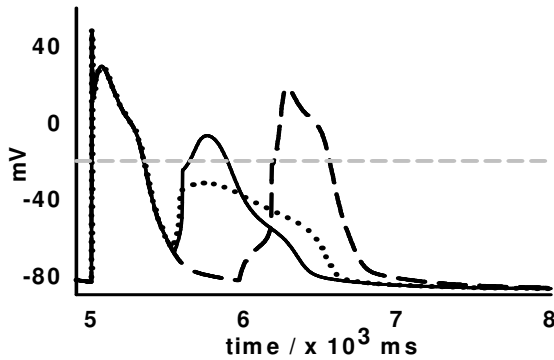
Fig 4. DAD in HF mid- case. 5 conditioning pulses (5th pulse shown) at 1 s interval were applied. Spontaneous release of Ca^{2+} simulated after 520 ms (dotted line), 535 ms (solid line), and after 960 ms (dashed line). DAD induced AP were defined as membrane potentials that exceeded -20 mV (grey dashed line).

calcium transient shows two different amplitudes, were observed. Bifurcation diagrams were constructed by plotting $[Ca^{2+}]_i$ amplitude against the BCL as shown in Fig. 3 for mid- cells. $[Ca^{2+}]_i$ alternans behaviour in NF was observed at or below a BCL of 438 ms in endo-, 415 in mid-, 424 in epi-. $[Ca^{2+}]_i$ alternans behaviour in HF was observed at or below a BCL of 805 ms in endo-, 1162 ms in mid-, and 706 ms in epi-.

DAD were simulated in all NF and HF cell models. There was no DAD-induced AP in the NF. DAD-induced AP were however observed in all three cases for HF. Such AP started to occur at 530 ms after SR Ca^{2+} release, and subsided at 980 ms in the HF mid- case. This is illustrated in Fig 4. Similar results were seen for the endo- and epi- cells.

CV was measured to be greatest in mid- strand (72 cm/s) among the three types of homogenous strands (71.12 cm/s for endo-, and 70.1 cm/s for epi-). An increase in CV was observed due to HF in all 3 types of homogenous tissue. CVr was obtained by methods described in the Methods. CVr for mid- 1-D tissue is shown in Fig 5. In NF, conduction block was seen to occur at DI of 377 ms (endo-), 421 ms (mid-) and 373 ms (epi-). In HF, we saw that conduction block occurs at 494 ms (endo-), 594 ms (mid-) and 482 ms (endo-).

VW in homogenous tissues was quantified by measuring the time window during which excitation wave by a premature stimulus can only propagate uni-directionally. In NF, the value was seen to be 1.7 ms (endo-), 2.6 ms (mid-), 1.7 (epi-). In the HF case, we saw that VW is increased and has values 2.6 (endo-), 3.9 ms(mid-) and 1.9 ms (epi-). The maximum change in VW due to HF was observed in the mid- tissue.

We investigated vulnerability of homogenous tissues due to DAD induced APs as described in the Methods. In NF, no vulnerability was observed as the DAD induced membrane excitation failed to initiate propagation. In HF the VW was 7 ms (endo-), 10 ms (mid-), 5 ms (epi). The minimum stimulation length required was 10 mm.

APD distribution after a solitary propagation on the transmural ventricular strand was measured to quantify the effects of HF on transmural AP heterogeneity. It was shown that the maximal APD difference in NF is 47.2 ms, was greater than 35.6 ms in HF.

Spatial distribution of vulnerability on the transmural ventricular strand was computed by measuring VW at each node of the the 15 mm long tissue in the NF and HF cases. This is shown in Fig. 6 where the time windows for uni-directional propagation are shown for each position along the 1-D virtual tissue. Although HF reduces AP heterogeneity, it increased the vulnerability of tissue to re-entry along the whole strand.
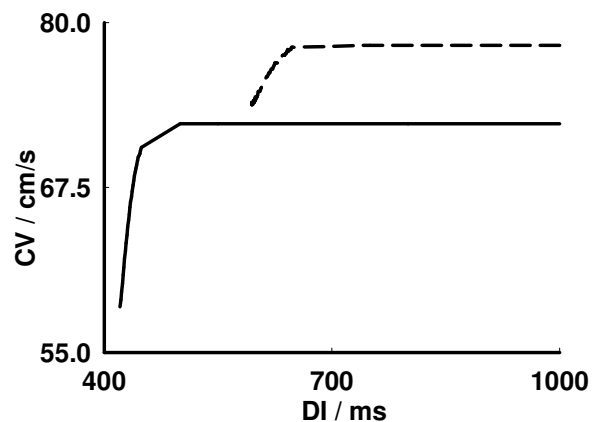
Fig 5. CVr for homogenous mid- 1-D tissue in NF (solid line) and HF (dashed line) cases.

4. Discussion and conclusions

In this study, our main findings are (i) APDr shows a steep and negative slope in HF. Negatively sloped restitution has been linked to instability of 2D spiral waves arrythmias in simple and physiologically detailed models [3]; (ii) HF shifts the genesis of AP and Ca^{2+} alternans to greater BCL region suggesting its pro-arrythmogenic effects, as the pro-arrythmogenic AP [10] or $[Ca^{2+}]_i$ alternans can occur at lower heart rates compared to NF; (iii) Most interesting is the existence of DAD-induced AP in HF and absence in NF. DAD-induced AP can form a conduction block or alter ventricular conduction that leads to re-entrant excitation; (iv) In HF, the measured VW in homogenous tissues are greater than in the NF tissues. This can be attributed to

the HF-induced prolongation of APD; (v) While decreasing the transmural APD heterogeneity, HF augments the vulnerability of tissue to re-entry. Details of mechanisms require further studies.
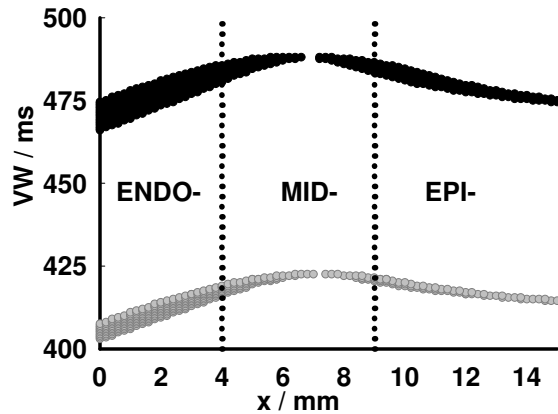
 Fig 6. Vulnerability in transmural of NF (dark circles) and HF (grey circles). The time interval during which uni-directional propagation was observed is plotted as a function of position.

Acknowledgements

References

[1]   Ebinger MW, Krishnan S, Schuger CD. Mechanisms of ventricular arrythmias in heart failure. Curr. Heart Fail. Rep. 2005; 2 (3): 111-117.

[2]   Preibe, L, Beuckelmann D J. Simulation study of cellular electric properties in heart failure. Circ. Res. 1998; 82: 1206-1223.

[3]   Bernus O, Verschelde H, Panfilov AV. Spiral wave stability in cardiac tissue with biphasic restitution. Phy. Rev. E. 2003; 68: 21917.

[4]   Panfilov AV, Zemlin CW. Wave propagation in an excitable medium with negatively sloped restitution curve. Chaos 2002; 12(3): 800-806.

[5]   Kharche S, Zhang H, Clayton RC, Holden AV. Simulation of hypertrophy in rat left ventricular cells. Computers in Cardiology 2004; 31: 513-516.

[6]   Zhang H, Garratt CJ, Zhu JJ, Holden AV. Role of upregulation of $I(K,1)$ in action potential shortening associated with atrial fibrillation in human. Cardiovas. Res. 2005; 66: 493-502.

[7]   Shiferaw Y, Sato D, Karma A. Coupled dynamics of voltage and calcium in paced cardiac cells. Phys. Rev. E Stat. Nonlin. Soft. Matter Phys. 2005; 71: 21903.

[8]   Bernus O, Wilders R, Zemlin CW, Verschelde H, Panfilov AV. A computationally efficient electrophysiological model of human ventricular cells. Am. J. Physiol. 2002; 282(6): H2296-2308.

[9]   Biktashev VN, Holden AV. Re-entrant waves and their elimination in a model of mammalian ventricular tissue. Chaos 1998; 8(1): 48-56.

[10] Wanatabe M, Koller M. Mathematical analysis of dynamics of cardiac memory and accommodation: theory and experiment. Am. J. Physiol. 2002; 282: H1534-H1547.

Address for correspondence

Sanjay Kharche
Biological Physics Group
School of Physics and Astronomy
Sackville Street Building
Sackville Street
The University of Manchester
Manchester M60 1QD
UK
Sanjay.Kharche@manchester.ac.uk